Journal of Pain Research

Dovepress
open access to scientific and medical research

Open Access Full Text Article

ORIGINAL RESEARCH

Peripheral drive in Aα/β-fiber neurons is altered in a rat model of osteoarthritis: changes in following frequency and recovery from inactivation

This article was published in the following Dove Press journal:
Journal of Pain Research
15 March 2013
Number of times this article has been viewed

Qi Wu
James L Henry

Department of Psychiatry and Behavioral Neurosciences, McMaster University, Hamilton, ON, Canada

Purpose: To determine conduction fidelity of Aα/β-fiber low threshold mechanoreceptors in a model of osteoarthritis (OA).

Methods: Four weeks after cutting the anterior cruciate ligament and removing the medial meniscus to induce the model, in vivo intracellular recordings were made in ipsilateral L4 dorsal root ganglion neurons. L4 dorsal roots were stimulated to determine the refractory interval and the maximum following frequency of the evoked action potential (AP). Neurons exhibited two types of response to paired pulse stimulation.

Results: One type of response was characterized by fractionation of the evoked AP into an initial nonmyelinated-spike and a later larger-amplitude somatic-spike at shorter interstimulus intervals. The other type of response was characterized by an all-or-none AP, where the second evoked AP failed altogether at shorter interstimulus intervals. In OA versus control animals, the refractory interval measured in paired pulse testing was less in all low threshold mechanoreceptors. With train stimulation, the maximum rising rate of the nonmyelinated-spike was greater in OA nonmuscle spindle low threshold mechanoreceptors, possibly due to changes in fast kinetics of currents. Maximum following frequency in Pacinian and muscle spindle neurons was greater in model animals compared to controls. Train stimulation also induced an inactivation and fractionation of the AP in neurons that showed fractionation of the AP in paired pulse testing. However, with train stimulation this fractionation followed a different time course, suggesting more than one type of inactivation.

Conclusion: The data suggest that joint damage can lead to changes in the fidelity of AP conduction of large diameter sensory neurons, muscle spindle neurons in particular, arising from articular and nonarticular tissues in OA animals compared to controls. These changes might influence peripheral drive of spinal excitability and plasticity, thus contributing to OA sensory abnormalities, including OA pain.

Keywords: dorsal root ganglion, repetitive firing, peripheral drive, electrophysiology, conduction failure, adaptation

Introduction

Osteoarthritis (OA) is the most common type of arthritis, afflicting approximately 10% of the population. The most intractable medical need in the management of OA is pain, along with other psychoneurological symptoms, such as fatigue and impaired proprioceptive performance. Unfortunately, how OA pain is initiated and maintained remains largely unknown, although joint nociceptors have long been proposed as the source of the pain.[1,2]

Correspondence: James L Henry
Department of Psychiatry and Behavioral Neurosciences, 1280 Main St West, HSC 4N35, McMaster University, Hamilton, ON L8S 4K1, Canada
Tel +1 905 525 9140 ext 27751
Email jhenry@mcmaster.ca

Recently, evidence was provided in a surgically induced rat model of OA that there are significant changes in the configuration of evoked action potentials (APs) in non-nociceptive Aα/β-fiber low threshold mechanoreceptors (LTMs) recorded intracellularly in the dorsal root ganglion (DRG) yet only minor changes in either C- or Aδ-fiber nociceptors at a stage when both structural loss and pain were confirmed in the model.[3] This raises the possibility of a role of Aα/β-fiber non-nociceptive primary sensory neurons in the pathogenesis of OA pain. In Aα/β-fiber LTMs, changes in configuration of the AP are associated mainly with the rising phase of the AP, suggesting a possible involvement of sodium channels.[3] These changes mainly reflect the passive properties of sodium channels during AP genesis in these neurons.

How Aα/β-fiber LTMs behave in dynamic situations, such as in response to repetitive stimulation, is an important issue as this would affect how peripheral signals to the central nervous system are coded. Peripheral drive from primary sensory neurons has been suggested to play an important role in developing and maintaining spinal plasticity, or central sensitization.[4–8] Primary sensory neurons thus contribute to changes in excitability and to plasticity of second order spinal neurons, partly via frequency-dependent modulation of synaptic transmission to these neurons.[9–12] Recent evidence shows that in sensory neurons repetitive stimulation causes AP broadening and prolonged refractory periods,[13] which could impart a memory of previous neuronal activity and thereby improve precision of the response and information transfer.[14,15]

Potassium and calcium ionic mechanisms have been proposed to explain conduction failure due to changes in refractoriness during repetitive stimulation.[16–18] Inactivation of sodium currents following successive APs has also been shown to contribute to activity-dependent AP adaption and therefore partially governs the fidelity of AP conduction.[19–22] The present study was a development from the authors' previous study in which Aα/β-fiber LTMs were proposed to play a role in OA pain and changes in sodium currents were also implied.[3] Therefore, the present study was restricted to examining sodium current-related properties of the AP in Aα/β-fiber LTMs in response to repetitive stimulation.

There are two basic forms of inactivation of sodium channels, fast and slow, each with distinct dynamics. The former occurs during the AP and is largely governed by the voltage sensing S4 segment of the sodium channel, whereas the latter can last tens of seconds and is regulated by auxiliary β-subunits.[23] It was hypothesized that there are significant alterations in the dynamic properties of sodium channels in large diameter LTM neurons in the surgically induced knee derangement model of OA.

Material and methods

All experimental procedures were approved by the McMaster University Animal Review Ethics Board and conform to the Guide to the Care and Use of Laboratory Animals of the Canadian Council of Animal Care, Volumes One and Two. At the end of the acute electrophysiological experiment each animal was euthanized without recovery from anesthesia by an overdose of the anesthetic.

Surgical induction of the model

Details of the induction of the animal model of OA, animal preparation for acute electrophysiological recording and in vivo intracellular recording have been published.[24] Briefly, female Sprague Dawley rats (180–225 g) from Charles River Laboratories (Wilmington, MA, USA) were used. Rats were anesthetized with a mixture of ketamine–xylazine and acepromazine (5 mL ketamine [100 mg/mL], 2.5 mL xylazine [20 mg/mL], 1.0 mL acepromazine [10 mg/mL], 1.5 mL sterile saline) at the dose of 0.1 mL/100 g body weight, injected intramuscularly. When the animals had attained a surgical level of anesthesia the medial meniscus was removed, and the anterior cruciate ligament was cut. The incision was then sutured in two layers. After surgery the animals were given 0.05 mL of the antibiotic Novo-Trimel® (trimethoprim sulfamethoxazole; 0.1 mL/100 mg; Novopharm, Toronto, ON, Canada) and 0.05 mL of the analgesic Temgesic® (buprenorphine; Schering-Plough, Kenilworth, NJ, United States), and allowed to recover from anesthesia before being returned to their home cage. Over the first 3 days postoperation, the animals were given daily doses of Novo-Trimel and Temgesic. Naïve animals served as controls.

Acute experimental setup

One month after model induction the animal was anesthetized as above and the right jugular vein was cannulated for intravenous infusion of drugs. A laminectomy was performed to expose the L4 DRG ipsilateral to the surgical derangement. The animal was fixed and suspended in a stereotaxic frame. The exposed spinal cord and DRG were covered with warm paraffin oil to prevent drying. The dorsal root of the L4 DRG was cut close to the spinal cord to allow a 12–15 mm length for electrical stimulation, and one pair of bipolar platinum stimulating electrodes was placed underneath.

Rectal temperature was maintained at 37°C with a servo-controlled infrared lamp, and the animal was mechanically ventilated to achieve an end-tidal carbon dioxide concentration around 40 mmHg. An initial 1 mg/kg dose of pancuronium (Sandoz International GmbH, Holzkirchen, Germany) was given to eliminate muscle tone. The effect of pancuronium persisted for approximately 1 hour; it was allowed to wear off periodically in order to confirm a surgical level of anesthesia, as judged by pupil dilation and any withdrawal from a pinch to a forelimb. Supplements of pentobarbital (Ceva Sante Animale, Libourne, France; 20 mg/kg) were added as needed to maintain a surgical level of anesthesia; generally, supplements of pentobarbital and pancuronium (one-third of the initial dose) were given every hour.

In vivo intracellular recording

Intracellular recordings from somata in the L4 DRG were made with micropipettes fabricated from filament-containing borosilicate glass tubing filled with 3 M potassium chloride solution, with direct current resistance 40–70 MΩ. The microelectrode was advanced by an EXFO IW-800 micromanipulator (EXFO, Quebec, QC, Canada). Intracellular recording was established when a hyperpolarization of at least –40 mV suddenly occurred and an AP could be evoked by electrical stimulation of the L4 dorsal root. Evoked APs were recorded with a Multiclamp™ 700B amplifier (Molecular Devices, Sunnyvale, CA, USA) and digitized online via a Digidata® 1322A interface (Molecular Devices) with pCLAMP™ 9.2 software (Molecular Devices).

Scope of the study and neuronal type involved

A pilot study had shown that C- and Aδ-fibers fail quickly in response to repetitive stimuli, even to paired pulse stimuli. These small diameter neurons fired only a limited number of APs to stimulus pairs or trains and then became unresponsive throughout the rest of the stimulation period. This made it impossible to obtain reliable measurements of recovery. Therefore, the present study was limited to Aα/β-fiber neurons, which are relatively resistant to failure in response to repetitive stimuli.

Sensory receptive properties of neurons were identified by various mechanical stimuli, and classified as previously described.[25] The criteria for an Aα/β-fiber neuron were based mainly on dorsal root conduction velocity, which was faster than 6.5 m/second.[26] To identify the receptive field and sensory properties of Aα/β-fiber LTMs, forces induced by a moving brush, blunt probes, and light tapping were applied on the ipsilateral lower extremity. Subcutaneous afferents were differentiated from cutaneous afferents by the stability of the response when the skin was lifted away from subcutaneous structures. The neurons recorded included various subtypes, such as guard hair, field hair, Pacinian, glabrous rapidly adapting, slowly adapting Types I and II, and muscle spindle Types I and II. Guard and field hair neurons, both rapidly adapting cutaneous hair units responding to light brush or touch on the skin, were grouped together under the category of hair follicle neurons. Pacinian neurons responded best to tapping, but over a broad skin area. Glabrous rapidly adapting neurons responded only to stimulation on glabrous skin, and adapted rapidly. Slowly adapting neurons responded and adapted slowly to light tactile stimuli to the cutaneous receptive field. Subcutaneous afferents were classified as muscle spindle neurons if they had very low thresholds to gentle pressure against muscle tissue and/or showed ongoing discharge at a regular frequency.

Stimulation protocol

One pair of bipolar stimulating electrodes was placed under the L4 dorsal root. Stimuli were delivered antidromically along the dorsal root to elicit APs in the somata. The stimulation pulse was delivered from an S-940 Interface Adapter and S-910 Stimulus Isolation Unit (Dagan Corporation, Minneapolis, MN, USA). The stimulus strength was set to approximately two times the activation threshold. Based on pilot studies, the current strength was normally around 0.8 mA for dorsal root stimulation. In this and another previous study,[24] an AP evoked by dorsal root stimulation was considered a somatic (S)-spike when the resting membrane potential was more negative than –40 mV and the AP amplitude was greater than 40 mV. Thus, an evoked AP with an amplitude less than 40 mV or the loss of an evoked AP was considered conduction failure.

Paired pulse stimulation

To investigate the fast process of recovery from repetitive firing in each type of neuron, paired pulse stimuli were delivered to the dorsal root. As the interspike interval was gradually shortened, the AP began to fractionate; two components of the second spike became gradually separated on the rising phase of the AP. Paired pulse stimulation started with search sweeps with coarse interval steps at 0.2–1 milliseconds, followed with testing sweeps with finer interval steps of 0.1 milliseconds. Each stimulus pair was separated by a period of 4 seconds.

From each recording and its differentiated derivative, the duration, amplitude, and maximum rising rate (MRR) for various components of the second evoked spike were measured (Figure 1). For each neuron, the recording at refractory interval (RI) was chosen for these analyses. According to previous descriptions of the spike components following paired pulse stimulation,[27,28] these two components were named the nonmyelinated (NM)-spike, which is the initial small amplitude component elicited alone at shorter interstimulus intervals, and the later S-spike, which is the larger amplitude component. When the interstimulus interval was reduced, only the NM-spike component was elicited. The amplitude of the NM-spike component remains relatively constant, even when the S-spike component fails. At that interval only the NM-spike component remains.[27,28] Therefore, RI refers to the shortest interstimulus interval at which the second S-spike can be elicited.

It was speculated that the NM-spike component might represent the fast kinetics of tetrodotoxin (TTX)-sensitive sodium currents, whereas the S-spike component might represent the slow kinetics of TTX-sensitive sodium currents, rather than a difference between TTX-sensitive

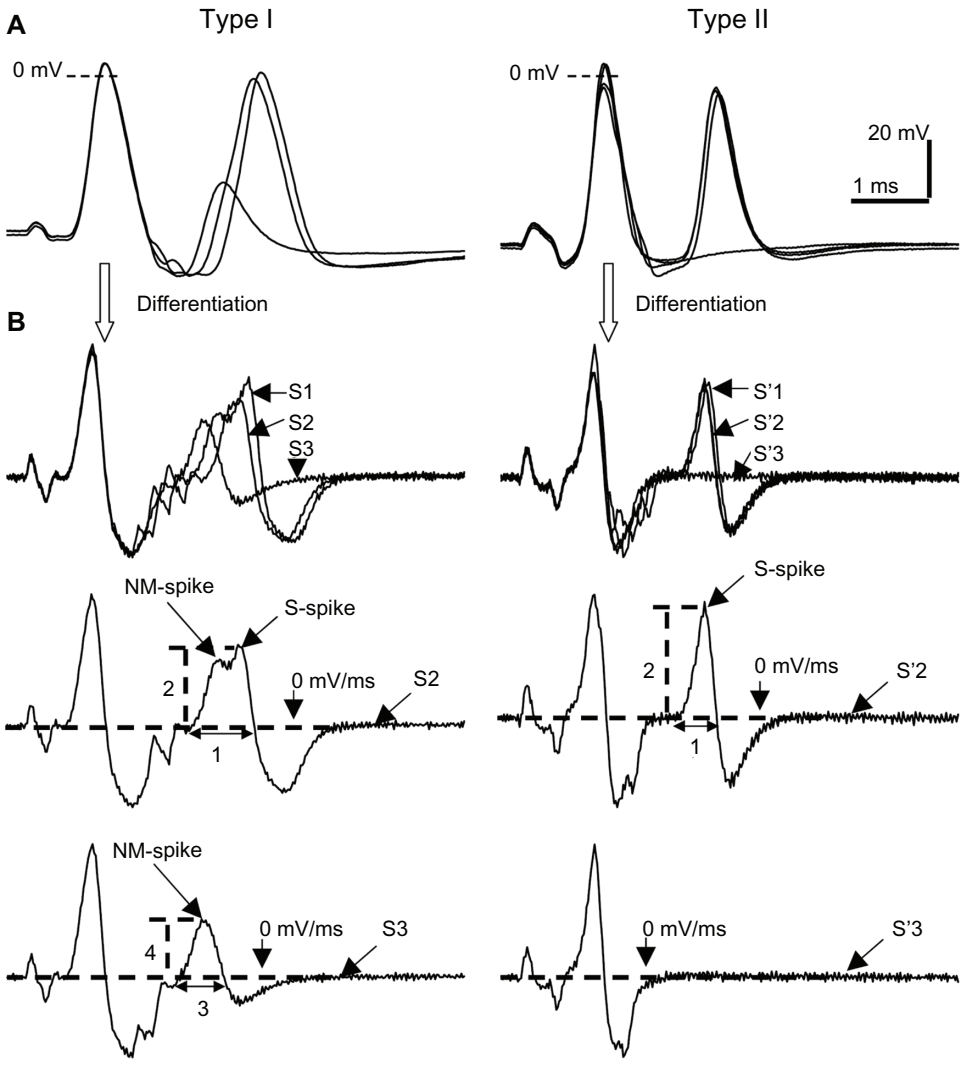

Figure 1 Types of response in Aα/β-fiber dorsal root ganglion neurons to paired pulse stimulation to dorsal roots. (**A**) Recordings from a glabrous rapidly adapting neuron (left panel) and muscle spindle neuron (right panel) stimulated with paired pulses of variable interstimulus intervals. These responses represent the two types of response to paired pulse stimulation in Aα/β-fiber neurons. The fractionating response is characterized by variable amplitude and fractionation of the second AP as it begins to fail at shorter intervals, whereas the all-or-none response is characterized by an all-or-none response of the second AP. (**B**) Differential derivatives of the respective recordings in Figure 1A.

Notes: The sweeps before and after failure of the second AP are shown separately. Left panels represent differentiated recordings and corresponding measurements typical of the fractionating type of response, and also show the NM-spike and the S-spike components and their dynamics during paired stimuli. The right panels represent those for the all-or-none type of response, in which no fractionation of the second spike was observed and only the S-spike component was seen. Parameters 1–4 are measurements of the rise time and the maximum rising rate of the second spike and the residual AP; S1–S3 represent the number of the stimulus pair as they are brought together.

Abbreviations: AP, action potential; NM, nonmyelinated; S, somatic.

and TTX-resistant currents. There are two reasons for this speculation. First, TTX-resistant currents are present only in a very small number of Aα/β-fiber LTMs,[29,30] which does not agree with the commonness of the "inflected second spike" in these neurons in the present study. Second, different TTX-sensitive sodium channel subtypes recover from inactivation at varying rates; $Na_v1.6$ recovers fastest, while $Na_v1.3$ and $Na_v1.7$ recover more slowly.[31,32]

The strategy to investigate the fast process of recovery from repetitive firing was twofold. First, to investigate the dynamics of the NM-spike component, measurements were recorded of the MRR and the amplitude of the AP where the S-spike component just starts to fail. MRR was measured as the peak voltage change over time from the differentiated derivative of the evoked AP. Second, to investigate the dynamics of the S-spike component that fails at shorter interstimulus intervals, the MRR and AP amplitude of the two evoked APs were compared with two parameters, the Paired Pulse MRR Index of Change and AP Amplitude Index of Change. The equations to calculate these two parameters are as follows:

$$\text{Paired Pulse MRR Index of Change} = \frac{\text{MRR of the second evoked AP}}{\text{MRR of the first evoked AP}}$$

$$\text{Paired Pulse AP Amplitude Index of Change} = \frac{\text{AP amplitude of the second evoked AP}}{\text{AP amplitude of the first evoked AP}}$$

The difference between neurons in control and OA animals was determined at arbitrary interstimulus intervals that are different between each neuronal type but are the same for each type of neuron. For example, hair follicle and Pacinian neurons were tested at an interval of 1 millisecond, glabrous rapidly adapting and slowly adapting neurons at 1.2 milliseconds, and muscle spindle neurons at 0.4 milliseconds. These interstimulus intervals were chosen in order to achieve the greatest "N," which were the most common stimulation intervals for each neuronal type in control and OA animals. A period as short as 4 seconds between successive paired stimuli was found sufficient to allow full recovery from the previous pair; measurements of each electrophysiological parameter of the first spike in each sweep remained constant, and were the same as those from single evoked AP under lower current strength.

Train stimulation: AP following frequency

To investigate the slow process of AP recovery from repetitive firing in each type of neuron a 200-millisecond stimulus train was delivered to the ipsilateral L4 dorsal root. Trains of stimuli at different frequencies were programmed using the pCLAMP protocol editor; train frequencies ranged from 40–1200 Hz. The frequency of the stimulation train was increased gradually in steps of 30 Hz for stimulating Aα/β-fiber LTMs. A period of 4 seconds separated each sweep of train stimuli. Once the frequency of the train of stimuli exceeded the maximum frequency a neuron could follow, AP conduction failure began to appear.

An AP Following Index was determined for each neuron with the following equation:

$$\text{AP Following Index} = \frac{\text{Number of APs evoked by the train pulse}}{\text{Stimulation frequency} \times 0.2}$$

This AP Following Index was plotted against a range of stimulation frequencies (Figure 2A), and then this plot was fitted with a single exponential decay function. To standardize the calculation of the following frequency, the AP Following Indexes of 1.0, 0.8, and 0.5 were calculated from the fitted curve of each train pulse recording as shown in Figure 2B. Therefore, the maximum following frequency of a neuron is the maximum stimulation frequency at which the neuron followed every stimulus throughout a 200-millisecond train, ie, the stimulation frequency at the AP Following Index of 1.0.

Train stimulation: AP rising rate

The MRR amplitude of evoked APs in train pulse recordings was also found to gradually decrease, especially at higher stimulation frequencies. Besides the fast inactivation of sodium currents that is similar to what is observed in paired pulse stimulation, slow inactivation of sodium currents may offer another explanation for this phenomenon, as prolonged repetitive stimulation has been shown to induce slow inactivation of sodium currents.[33]

To quantify the decay in MRR during train stimulation, the Train Stimulation MRR Index of Change was used. It was calculated as follows:

$$\text{Train Stimulation MRR Index of Change} = \frac{\text{Average MRR of all APs evoked by a train}}{\text{MRR of the first evoked AP in the train pulse}}$$

First, the Train Stimulation MRR Index of Change at the maximum following frequency and Paired Pulse MRR Index of Change at corresponding interstimulus intervals were compared between neurons in control versus OA animals. Second, the

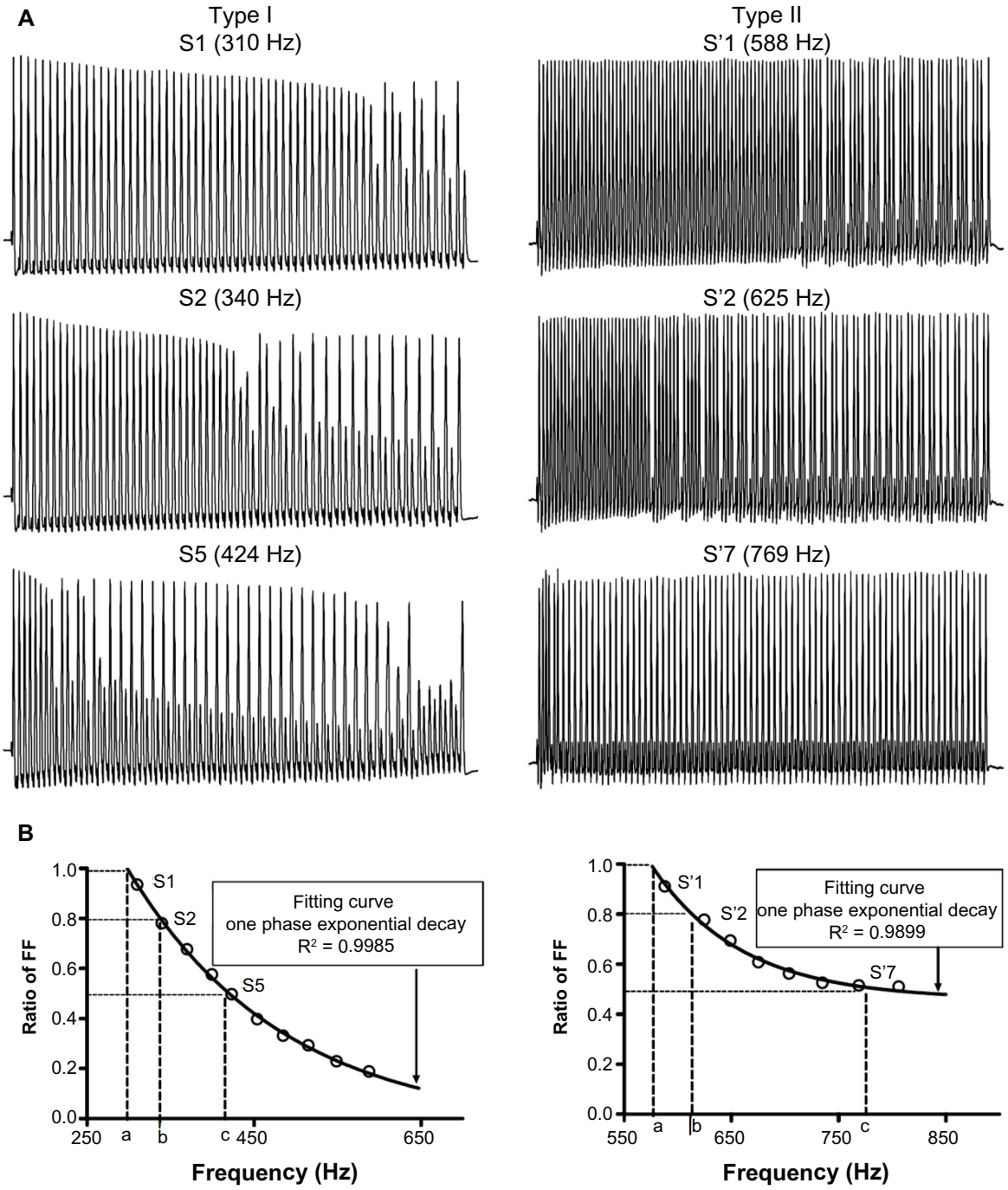

Figure 2 Patterns of response and measurements from recordings during train pulse stimulation of the dorsal root. (**A**) Actual recordings from a glabrous rapidly adapting neuron (left panel) and a muscle spindle neuron (right panel) stimulated with a 200-millisecond pulse train in order to demonstrate fractionating and the all-or-none types of response. Three selected recordings in each neuron (top, middle, and bottom in the panel) were sweeps with the Action Potential Following Index close to 1, 0.8, and 0.5, respectively. (**B**) The curves of frequency following from the recordings in the respective neurons stimulated with trains of different frequencies. It also shows that the maximum (a), 80% (b), and 50% (c) fiber FFs determined from the curve.

Notes: The curve of FF was plotted for a range of frequencies, which was later fitted with a one-phase exponential decay function. R^2 values shown represent the degree of fit.

Abbreviations: FF, following frequency; S, somatic.

difference in the Train Stimulation MRR Index of Change at the same stimulation frequency between neurons in control and OA animals was studied. The common stimulation frequencies for muscle spindle neurons were in the range of 515–588 Hz, and 280–340 Hz for the other types of Aα/β-fiber LTMs.

Statistical analysis

Numerical data are presented as mean ± standard error of the mean. For two group comparisons between the control and OA animals, Student's *t*-test was used for data showing normal distribution confirmed by the D'Agostino and Pearson

omnibus normality test. The Mann–Whitney *U* test was used for those not normally distributed. All tests and graphing were done using Prism® 4 software (GraphPad Software, Inc, La Jolla, CA, USA). The *P*-values of the *t*-tests are indicated in the figures, where appropriate. $P < 0.05$ was set as the level of statistical significance.

Results

During repetitive stimulation, such as paired pulse stimulation and train stimulation, evoked APs fractionated into NM-spike and S-spike components, as described in previous studies of conduction failure in DRG neurons.[16,28,34–39]

Patterns of response to repetitive stimuli in Aα/β-fiber neurons in control animals

In the present study, there were two basic types of response to repetitive stimulation. In one case the AP fractionated as the interstimulus interval was shortened, and in the other as the interstimulus interval was shortened the evoked AP failed altogether. Representative recordings of each type of response are shown in Figures 1 and 2.

In the case of the fractionating response, the second evoked AP is characterized as having an inflection on the rising phase as the interstimulus interval was shortened. As the interstimulus interval was shortened further, this second spike resolved into two components. In corresponding differentiated derivatives, these two spike components on the rising phase became gradually separated as the interval was gradually shortened. At these shorter interstimulus intervals the amplitude of the NM-spike component remained relatively constant, while the amplitude of the S-spike component decreased as the interstimulus interval was decreased. When the interval was short enough the second spike failed altogether, leaving only the NM-spike component. These properties are illustrated in the left column of Figure 1.

In neurons that exhibited fractionation in paired pulse stimulation, during stimulation with a 200-millisecond stimulus train, conduction failure of some of the APs occurred as the stimulation frequency was gradually increased, ie, as the interstimulus interval was gradually decreased. This conduction failure was observed as the absence of evoked APs and even of the NM-spike component. These properties are illustrated in the left column of Figure 2.

This fractionating type of response to repetitive stimulation was observed in the majority of naïve control hair follicle neurons (13/15), all glabrous rapidly adapting neurons (17/17), half of the Pacinian neurons (12/24), and about one-third of muscle spindle neurons (14/44).

In contrast, the all-or-none type of response is characterized as having no inflection on the rising phase of the second spike, and the abrupt failure of the second spike as the interstimulus interval was gradually shortened. This is illustrated in the right column of Figure 1. In the corresponding differentiated derivatives, no obvious separation of components on the rising phase is observed. When the interval was sufficiently short, the second evoked AP was completely abolished, without any partial AP, such as that illustrated in the left column of Figure 1.

During train stimulation, conduction failure was manifested as the sudden complete absence of evoked APs at the higher frequencies. This is illustrated in the right column of Figure 2. An all-or-none type response to repetitive stimulation was observed in the majority of naïve control muscle spindle neurons (28/44), half of the Pacinian neurons (12/24), and a few hair follicle neurons (2/15).

Fast inactivation during paired pulse stimulation in control versus OA animals

The refractory period of a neuron limits the rate at which the neuron can maximally discharge APs. The RI is a measure of this refractory period, which limits the rate of firing. Mechanisms regulating the duration of this refractory period include mainly the recovery of sodium currents from inactivation following an AP as well as the activation of potassium currents.

In naïve control animals to determine the RI, the dorsal root of each neuron was stimulated antidromically with ~0.8 mA constant current. Muscle spindle neurons, which normally have ongoing discharge, had the shortest RI (0.52 ± 0.051 milliseconds, N = 44). Other types of Aα/β-fiber non-nociceptor had an intermediate RI, including hair follicle neurons (1.08 ± 0.131 milliseconds; N = 15), glabrous rapidly adapting neurons (0.96 ± 0.082 milliseconds; N = 17), slowly adapting neurons (0.96 ± 0.082; N = 4), and Pacinian neurons (0.77 ± 0.06 milliseconds; N = 24) (Figure 3).

In OA animals under the same stimulation conditions, RIs in pooled Aα/β-fiber LTMs were significantly shorter (0.74 ± 0.041 milliseconds, N = 104 in control versus 0.64 ± 0.042 milliseconds, N = 112 in OA animals; $P = 0.044$, Mann–Whitney *U* test). Among these subclasses of Aα/β-fiber LTMs, muscle spindle neurons exhibited the greatest difference. RIs in muscle spindle neurons in OA animals were significantly shorter (0.52 ± 0.051 milliseconds, N = 44 in control versus 0.31 ± 0.032 milliseconds, N = 47 in OA animals; $P = 0.003$, Mann–Whitney *U* test) (Figure 3). Any differences in the other types of Aα/β-fiber LTMs did not reach statistical significance (Table 1).

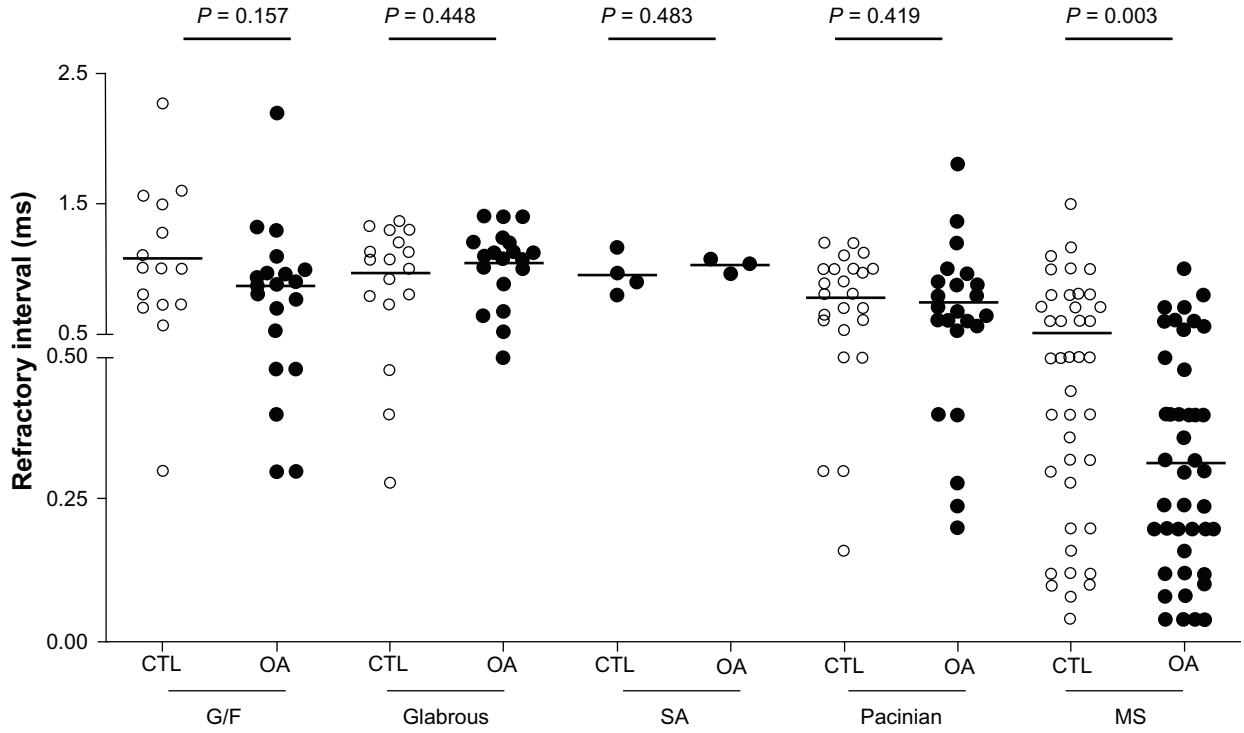

Figure 3 Refractory intervals in Aα/β low threshold mechanoreceptors in OA versus CTL.
Notes: In each case the median (horizontal line) is superimposed. Refractory intervals in various neuronal types (G/F neurons, glabrous rapidly adapting neurons, SA neurons, Pacinian neurons, and MS neurons) are shown, and the comparison between OA and CTL is shown for each neuron type. Each dot represents a recording from one neuron.
Abbreviations: CTL, control animals; G/F, guard and field hair; MS, muscle spindle; OA, osteoarthritis; SA, slowly adapting.

In order to investigate possible sodium mechanisms accountable for the shorter RI in OA Aα/β-fiber LTMs, the MRR of the NM-spike component (fast kinetic component) and the S-spike component (slow kinetic component) were measured. During paired pulse stimulation, an inflection on the rising phase of the second spike could be identified in 44/104 Aα/β-fiber LTMs in control animals (mainly nonmuscle spindle neurons, including five muscle spindle neurons) and 46/112 Aα/β-fiber LTMs in OA animals (including four muscle spindle neurons). MRR of the NM-spike component was measured from the AP in the sweep where the S-spike component just failed to appear, and was 107.71 ± 3.082 mV/millisecond in control animals (N = 44), which was significantly smaller than in OA Aα/β-fiber LTMs (122.72 ± 4.021 mV/millisecond, N = 46; $P = 0.004$, Student's *t*-test; Figure 4, right panel). However, no difference was found between the control and OA Aα/β-fiber LTMs in the amplitude of the NM-spike component (23.11 ± 0.881 mV,

Table 1 Refractory intervals and following frequencies in subtypes of Aα/β-fiber low threshold mechanoreceptor

Neuronal types	Refractory interval (ms)		*P*-value	Max following frequency (Hz)		*P*-value
	Control	OA		Control	OA	
G/F	1.08 ± 0.131 N = 15	0.86 ± 0.097 N = 20	0.157	343.2 ± 25.62 N = 13	367.3 ± 22.01 N = 17	0.259
Glabrous	0.96 ± 0.082 N = 17	1.04 ± 0.064 N = 19	0.448	353.6 ± 25.17 N = 15	333.1 ± 22.18 N = 16	0.545
Pacinian	0.77 ± 0.060 N = 24	0.74 ± 0.078 N = 23	0.419	355.8 ± 28.73 N = 21	443.6 ± 25.34 N = 21	*0.027
SA	0.96 ± 0.076 N = 4	1.03 ± 0.035 N = 3	0.483	341.2 ± 43.83 N = 4	392.4 ± 28.95 N = 2	0.495
MS	0.52 ± 0.051 N = 44	0.31 ± 0.032 N = 47	*0.003	574.6 ± 19.12 N = 35	632.1 ± 14.22 N = 38	*0.017

Notes: Values are given in Mean ± SE, and N = sample size. * indicates a statistical significance. "G/F", "Glabrous", "Pacinian", "SA", and "MS" represent hair follicle neurons, glabrous rapidly adapting neurons, Pacinian neurons, slowly adapting neurons, and muscle spindle neurons, respectively.
Abbreviation: OA, osteoarthritis.

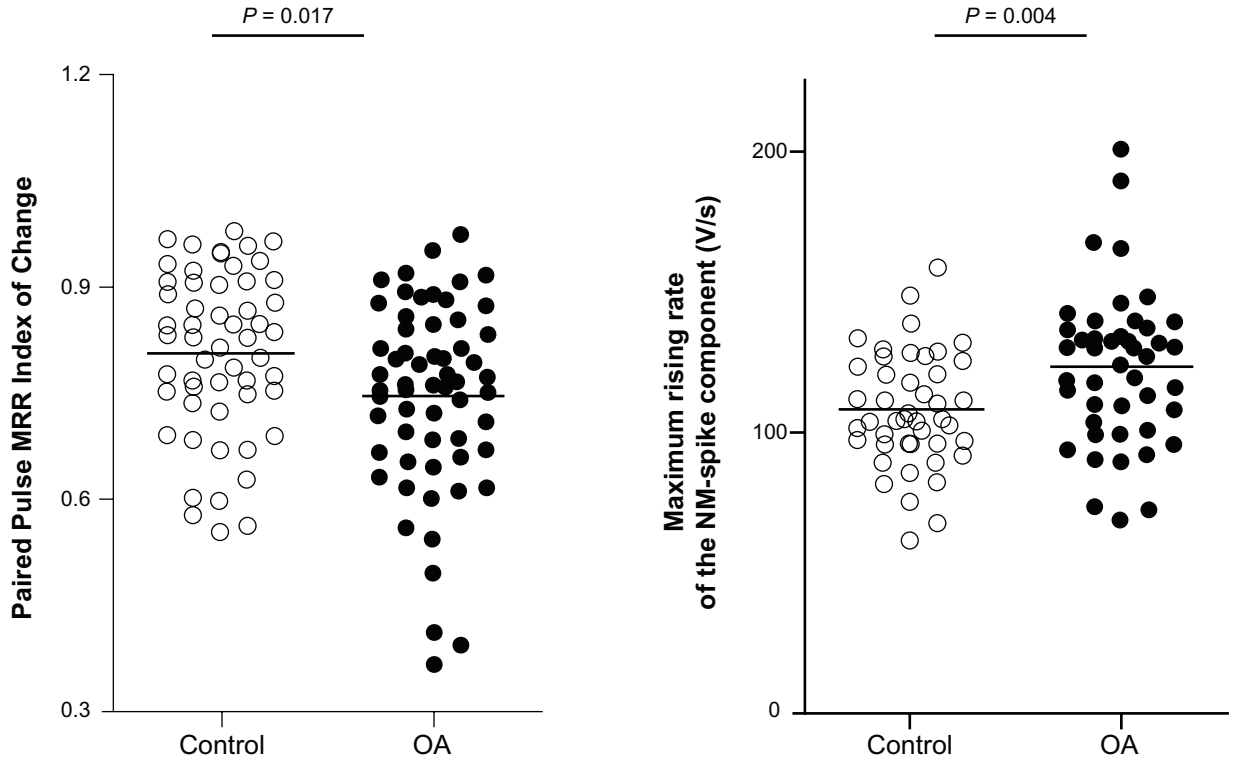

Figure 4 Changes in the MRR of the evoked action potentials during paired pulse stimulation in Aα/β low threshold mechanoreceptors in OA versus control animals.
Notes: In each case the median (horizontal line) is superimposed. MRR of the somatic-spike component (left panel) and of the NM-spike component (right panel) of the second evoked action potential during the paired pulse stimulation was compared between Aα/β low threshold mechanoreceptors in control versus OA animals. Left panel: the Paired Pulse MRR Index of Change was greater in OA than in control animals (N = 54 in control versus N = 60 in OA animals, Mann–Whitney *U* test). Right panel: the MRR of the NM-spike was greater in OA animals compared with control animals (N = 44 in control versus N = 46 in OA animals, Student's *t*-test). Each dot represents a recording from one neuron.
Abbreviations: MRR, maximum rising rate; NM, nonmyelinated; OA, osteoarthritis.

N = 44 in control versus 25.14 ± 1.082 mV, N = 46 in OA; $P = 0.132$, Student's *t*-test).

The amplitude of the S-spike component in neurons exhibiting a fractionation response gradually decreased as the interstimulus interval approached the interval at which failure of this component occurred. In order to optimize measuring the effect of shortening the interstimulus interval on the S-spike component, the amplitude of this component was measured at an arbitrary interval of 1.2 milliseconds. By doing so, a greater number of reliable recordings was yielded, 54/104 recordings in control Aα/β-fiber LTMs (including five muscle spindle neurons) and 60/112 recordings in OA Aα/β-fiber LTMs (including ten muscle spindle neurons). The Paired Pulse MRR Index of Change was significantly smaller in OA Aα/β-fiber LTMs (0.81 ± 0.016, N = 54 in control versus 0.75 ± 0.017, N = 60 in OA animals; $P = 0.017$, Mann–Whitney *U* test; Figure 4, left panel). Moreover, the Paired Pulse AP Amplitude Index of Change was significantly smaller in OA Aα/β-fiber LTMs compared to control counterparts (0.94 ± 0.007, N = 51 in control versus 0.9 ± 0.008, N = 60 in OA animals; $P = 0.003$, Mann–Whitney *U* test).

Therefore, in OA animals, RI measurement and further MRR analyses revealed various signs of an altered fast recovery from paired pulse stimulation in distinct subclasses of Aα/β-fiber LTMs: shorter RI in muscle spindle neurons, greater MRR of the NM-spike component, and smaller MRR of the S-spike component of the second evoked AP in nonmuscle spindle neurons.

Slow inactivation during train stimulation in control versus OA animals

In control animals the maximum following frequency for each type of neuron was as follows: slowly adapting neurons 341.2 ± 43.81 Hz (N = 4); hair follicle neurons 343.2 ± 25.62 Hz (N = 13); glabrous rapidly adapting neurons 353.6 ± 25.22 Hz (N = 15); Pacinian neurons 355.8 ± 28.73 Hz (N = 21); and muscle spindle neurons 574.6 ± 19.12 Hz (N = 35) (Figure 5).

The greatest difference in maximum following frequency comparing control and OA animals was in Pacinian neurons (355.8 ± 28.73 Hz, N = 21 in control versus 443.6 ± 25.32 Hz, N = 21 in OA animals; $P = 0.027$; Figure 5) and muscle

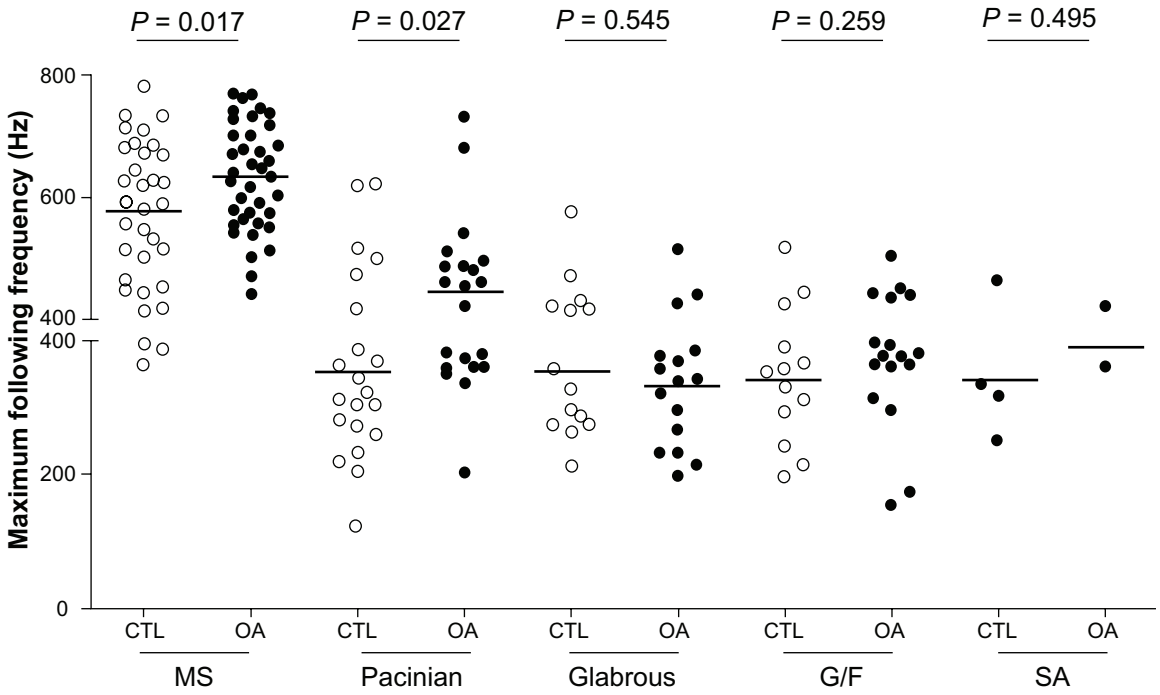

Figure 5 Maximum following frequency in Aα/β low threshold mechanoreceptors in OA versus CTL.
Notes: Maximum following frequencies are shown for various neuronal types (MS neurons, Pacinian neurons, glabrous rapidly adapting neurons, G/F neurons, and SA neurons), and are compared between OA and CTL for each type.
Abbreviations: CTL, control animals; G/F, guard and field hair; MS, muscle spindle; OA, osteoarthritis; SA, slowly adapting.

spindle neurons (574.6 ± 19.12 Hz, N = 35 in control versus 632.1 ± 14.22 Hz, N = 38 in OA animals, $P = 0.017$; Figure 5). In Aα/β-fiber LTMs in OA animals, there was a significantly greater maximum following frequency. The maximum following frequency was 440.0 ± 16.55 Hz in control animals (N = 88) and 486.1 ± 16.17 Hz in OA animals (N = 94; $P = 0.041$, Mann–Whitney U test). Differences in the other types of neurons did not reach the level of statistical significance (Table 1).

Importantly, the interstimulus interval of the train at which conduction failure began to occur was several times that of the RI as determined by paired pulse stimulation. This reflects the difference between slow inactivation observed during train stimulation, and fast inactivation which is observed during paired pulse stimulation. For example, the estimated shortest interstimulus interval in the train at the maximum following frequency was 2.9, 2.9, 2.8, 2.8, and 1.7 milliseconds in slowly adapting neurons, hair follicle neurons, glabrous rapidly adapting neurons, Pacinian neurons, and muscle spindle neurons, respectively. These values were 2.9, 2.6, 2.8, 3.5, and 3.4 times the respective RI as determined by the paired pulse stimulation. This suggests a summating inactivation effect developing slowly on spike electrogenesis during prolonged, repetitive AP generation evoked by the train stimulation.

Therefore, to determine whether or not the conduction failure in train stimulation was due to the limiting effect of the refractory period, the Train Stimulation MRR Index of Change at the maximum following frequency was compared with the Paired Pulse MRR Index of Change at corresponding interstimulus intervals (normally two to three times the RI). In control animals, 31 recordings were included in which the dorsal root was stimulated with trains in which interspike intervals were equivalent to two to three times the RI for each neuron. These neurons included five hair follicle neurons, nine Pacinian neurons, one glabrous rapidly adapting neuron, and 16 muscle spindle neurons. The Paired Pulse MRR Index of Change was 0.84 ± 0.016 (N = 31), which was significantly higher than the corresponding Train Stimulation MRR Index of Change (0.77 ± 0.007, N = 80; $P < 0.0001$, Student's t-test; Figure 6, left panel). This observation suggests an additional decay of the MRR, which might be due to other mechanisms besides the fast inactivation of sodium currents at play in paired pulse stimulation.

Next, to determine whether neurons in control versus OA animals were different with respect to the Train Stimulation MRR Index of Change, this index was compared at the same stimulation frequency between control and OA animals. The Train Stimulation MRR Index of Change in all control neurons combined in control animals was 0.83 ± 0.011

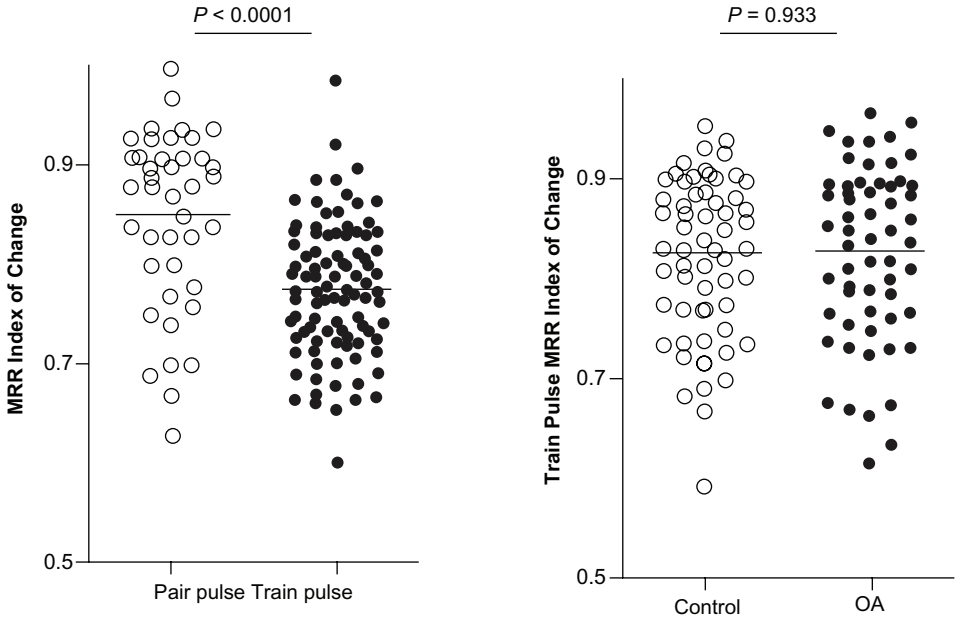

Figure 6 Changes in MRR of the evoked action potentials during train stimulation in Aα/β low threshold mechanoreceptors in OA versus control animals.
Notes: In each case the median (horizontal line) is superimposed. Left panel: the MRR Index of Change at similar refractory intervals was compared between paired pulse stimulation and train pulse stimulation in control animals. The Train Stimulation MRR Index of Change was smaller than the Paired Pulse MRR Index of Change (N = 31 of paired pulse recordings versus N = 80 of train pulse recordings, Student's *t*-test). Right panel: the Train Stimulation MRR Index of Change was measured in sweeps at the same selected stimulation frequencies in Aα/β-fiber low threshold mechanoreceptors in control and OA animals. There was no difference between control and OA animals (N = 60 in control versus N = 60 in OA animals, Student's *t*-test). Each dot represents a recording from one neuron.
Abbreviations: MRR, maximum rising rate; OA, osteoarthritis.

(N = 60), and was comparable to that in neurons in OA animals (0.83 ± 0.011, N = 60; $P = 0.933$, Student's *t*-test; Figure 6, right panel).

This part of the experiment did not support a role of the slow inactivation of sodium currents (at least for the slow kinetics of TTX-sensitive currents) in modulating the peripheral drive from Aα/β-fiber LTMs in OA animals, although the possible sodium current slow inactivation process did lead to a further decay in MRR in the train pulse stimulation compared to that in the paired pulse stimulation.

Discussion

The present study provides evidence of significant differences in peripheral drive in Aα/β-fiber LTMs in an animal model of OA compared to control animals. In vivo intracellular recording demonstrated that in OA animals the RI in paired pulse stimulation was shortened in muscle spindle neurons, and the maximum following frequency in train pulse stimulation was greater in Pacinian and muscle spindle neurons. Further, in paired pulse stimulation, MRR of the fast kinetics of NM-spike component was increased, while MRR of the slow kinetics of S-spike component was decreased in other nonmuscle spindle Aα/β-fiber LTMs in OA animals.

Muscle spindle neurons were the neuronal subtype most altered in peripheral drive. However, other nonmuscle spindle neuronal subtypes were also altered, although less markedly. This was evidenced by the observation that the kinetics of the second AP in a paired pulse protocol was altered in a mixed group of Aα/β-fiber LTMs mainly consisting of nonmuscle spindle neurons. Twice as many of the muscle spindle neurons were obtained in the present study compared to other neuronal subtypes, which might be a factor bias towards a statistically significant finding in muscle spindle neurons. Thus, it is possible to conclude that the importance of the data extends to the whole population of Aα/β-fiber LTMs.

These findings substantiate the previous suggestion that non-nociceptive Aα/β-fiber LTMs undergo significant functional changes in this animal model of OA.[3] This model was selected because physical injury is the most common cause of OA.[40] Further, a surgical model avoids introduction of chemicals such as the glycolysis inhibitor, monosodium iodoacetate, which may have widespread local effects. The surgical derangement model demonstrates many of the structural changes associated with OA, such as loss of joint cartilage and changes in subchondral bone microarchitecture and synovial proliferation.[41,42] Biochemical urinalysis profiles in this model correlate with the current understanding of OA pathology.[43] In addition, the model demonstrates a change in stance,[44] changes in chondrocyte gene expression consistent with joint disease,[45] and the model

can be made more severe as a result of stressful exercise.[43] In fact, the origin of these neurons at sites outside the joint prompts the examination a possible functional relationship of these changes to the symptoms often reported by people with OA. This is particularly important given the focus of some research exclusively on sensory neurons innervating the joint in animal models of OA. Such studies neglect the reports from OA patients that pain is referred to areas beyond the joint,[46,47] and the reported prevalence of pain even months or years after total joint replacement.[48] Instead, it is proposed that joint damage can lead to changes in the functional properties of large diameter sensory neurons arising from articular as well as from nonarticular tissues. At least in some cases of OA, these neurons (not exclusive to joint afferents) collectively contribute to the sensory alterations reported by people with OA. This view would account better for the referred pain, the persisting pain after joint arthroplasty, and the loss of proprioception[44] that are clinical presentations of OA patients.

Implication for sensory input to the spinal cord

Further analysis of MRR of evoked APs during either paired pulse stimulation or train pulse stimulation revealed a shift toward fast kinetic changes. In the present study, greater maximum following frequencies for muscle spindle afferents, Pacinian afferents, and other Aα/β-fiber LTMs in OA animals imply that more APs from nerve terminals would successfully invade the somata of these neurons. These findings reflect an increase in the fidelity of impulse conduction towards spinal cord in myelinated fibers in OA animals.

The somata of primary sensory neurons are connected to the respective axon by a short stem axon, forming a T-shaped structure, a "T-junction." Due to this pseudounipolar geometrical feature, the somata of DRG neurons do not directly participate in the AP through-conduction toward the spinal cord. Amir and Devor concluded in a computational model of DRG A-neurons that regulating the degree of electrical excitability of the soma did not affect the safety of impulse conduction from the peripheral nerve, past the DRG, via the dorsal root to the spinal cord.[27] This conclusion, drawn from modeling normal DRG neurons, models neurons under normal physiological conditions and might not apply to neurons in various pathophysiological conditions. In Amir and Devor's computational modeling regulation of the sodium channel, density was restricted to soma and initial segments of the stem axon, which largely contradicts current evidence; sodium channel expression is highly dynamic and is regulated in both the soma and axon.[49] Although the molecular signals that regulate sodium channel isoform expression, trafficking, clustering, and maintenance in axons are mostly unknown, there is evidence showing that growth factors, such as nerve growth factor and glial derived neurotrophic factor, as well as Schwann cells are involved in regulating sodium channel expression.[50,51]

There is at least one condition where the increase in AP soma invasion could indicate an increase in the fidelity of impulse conduction along the axon towards the spinal cord where there were changes in the composition of sodium channel isoforms expressed both in the soma and axon. A neuropathic component has been suggested in this animal model of OA.[3] This condition, similar to other neuropathic conditions, might result in a Wallerian degeneration along the peripheral nerve where sodium channel expression in the axon is commonly dysregulated.[51] $Na_v1.6$ is the predominant sodium channel isoform expressed at nodes of Ranvier within peripheral and central myelinated fibers[49] and is critical for AP conduction along axons. Interestingly, the neuronal types that have undergone the greatest change in the present study express mainly TTX-sensitive sodium channel isoforms; in particular, muscle spindle and Pacinian afferents have been reported to abundantly express $Na_v1.1$ and $Na_v1.6$ sodium channels.[30]

It is generally accepted that an altered peripheral input modulates secondary or higher sensory processing,[6] although detailed mechanisms remain elusive for most chronic disease conditions. In previous reports on this animal model of OA, various behavioral and/or sensory changes have been documented, including decreased hind paw withdrawal threshold, shorter tail withdrawal latency,[3] and altered hind limb weight bearing pattern.[44] However, it is not feasible to establish how a specific change in RI or maximum following frequency in muscle spindle neurons or nonmuscle spindle neurons is linked to a specifically altered function, eg, nociception or proprioception. Yet, with regard to the most affected neuronal subtype in the model of OA, the muscle spindle neuron, it is suggested that changes in these neurons might have complex functional implications, such as a loss of the original function (eg, as a proprioceptor), a gain of a novel function (eg, as a new input to a central network of nociception), or even possibly a combination of both. Further, it would be relevant in future studies to determine whether there are phenotypic changes in muscle spindle neurons and other nonmuscle spindle Aα/β-fiber LTMs, and/or a "rewiring" of central sensory pathways in OA.

Ionic mechanisms for increased soma invasion of the AP in Aα/β-fiber LTMs in OA

Changes in the rising phase of the AP as observed in the present study could largely be explained by changes in sodium ion mechanisms. However, the participation of potassium currents, especially in defining refractory periods, could not be precluded, as voltage- or calcium-dependent potassium channels have been suggested to account for neuronal properties in multiple spiking, such as refractory periods, maximum attainable frequency of spike discharge, and conduction failure.[13,52,53]

Two spike components could be observed at shorter interstimulus intervals in the present study. As indicated by previous in vivo and in vitro studies on the distribution of voltage-gated sodium channel subunits in subgroups of DRG neurons,[26,30,54–57] this suggests the existence of two or more sodium currents with different recovery kinetics that collectively generate the depolarization phase of the evoked AP in Aα/β-fiber LTMs, at least in neurons with Type I response.

The observation of an increase in the MRR of the NM-spike component and the decrease in the MRR of the S-spike component of Aα/β-fiber LTMs in OA animals compared to those in control animals might be due to either an increase in the absolute number of, or to an increase in recovery kinetics, of the fast kinetics of TTX-sensitive sodium channels, and that there were less slow kinetics of TTX-sensitive sodium currents remaining in the second spike after recovery from the first evoked AP in these neurons. As a result, a shortened RI in Aα/β-fiber LTMs in OA animals might be due to a shift toward more prominent fast kinetics of TTX-sensitive currents in these neurons, such as $Na_v1.6$, the fastest recovering sodium channel subtype. Another possibility is the re-expression of the fast priming embryonic TTX-sensitive $Na_v1.3$, as documented in animal models of neuropathy.[30,58,59] The expression of $Na_v1.3$ channels in DRG neurons has yet to be studied in OA models.

The minimum interval defining the maximum following frequency is 1.5–2.8 milliseconds in Aα/β-fiber LTMs. During the shortest interstimulus intervals, the recovery from fast inactivation is not complete for TTX-sensitive currents, as TTX-sensitive sodium currents recover slowly and remain incomplete 4 milliseconds following maximal inactivation.[60] The data show that a train of stimuli effectively promotes slow inactivation of sodium currents. It has been reported that inducing voltage-gated sodium channels into a slow inactivation state by therapeutic agents, such as lacosamide, casts a broad spectrum suppressive effect on mechanical and thermal hypersensitization in various chronic pain syndromes,[61] and is also effective in relieving chronic muscle pain, a common symptom in OA.[62] However, the data do not support a role of slow inactivation of sodium currents in the increased maximum following frequency in Aα/β-fiber LTMs in this OA model. This increase in maximum following frequency might be due to the same mechanism responsible for the shortened RI.

Conclusion

This study sets itself apart from previous studies on OA models that focus only on articular nociceptors and report changes in these neurons only. The present study provides evidence of functional changes in Aα/β-fiber low threshold DRG neurons in a derangement model of OA. The present study also presents evidence that there are changes in functional properties of neurons that innervate other structures beyond the joint. The data imply an altered peripheral drive towards spinal cord that might contribute to spinal plasticity and central sensitization.

Acknowledgments

This work was generously supported by the Canadian Arthritis Network, the Canadian Institutes of Health Research, and McMaster University. JLH was Chair in Central Pain in the Faculty of Health Sciences at McMaster University. QW was a Canadian Institutes of Health Research Strategic Training Fellow in Pain: Molecules to Community, and was supported by the Canadian Pain Society, Canadian Arthritis Network, and the Canadian Institutes of Health Research. The authors thank Mrs Chang Ye for help in data input and statistical analysis.

Disclosure

The authors report no conflicts of interest in this work.

References

1. Felson DT. The sources of pain in knee osteoarthritis. *Curr Opin Rheumatol*. 2005;17(5):624–628.
2. McDougall JJ. Pain and OA. *J Musculoskelet Neuronal Interact*. 2006; 6(4):385–386.
3. Wu Q, Henry JL. Changes in Aβ non-nociceptive primary sensory neurons in a rat model of osteoarthritis pain. *Mol Pain*. 2010;6:37.
4. Dalal A, Tata M, Allegre G, Gekiere F, Bons N, Albe-Fessard D. Spontaneous activity of rat dorsal horn cells in spinal segments of sciatic projection following transection of sciatic nerve or of corresponding dorsal roots. *Neuroscience*. 1999;94(1):217–228.
5. Pitcher GM, Henry JL. Nociceptive response to innocuous mechanical stimulation is mediated via myelinated afferents and NK-1 receptor activation in a rat model of neuropathic pain. *Exp Neurol*. 2004;186(2): 173–197.

6. Pitcher GM, Henry JL. Governing role of primary afferent drive in increased excitation of spinal nociceptive neurons in a model of sciatic neuropathy. *Exp Neurol*. 2008;214(2):219–228.
7. Seltzer Z, Cohn S, Ginzburg R, Beilin B. Modulation of neuropathic pain behavior in rats by spinal disinhibition and NMDA receptor blockade of injury discharge. *Pain*. 1991;45(1):69–75.
8. Sotgiu ML, Biella G, Riva L. A study of early ongoing activity in dorsal horn units following sciatic nerve constriction. *Neuroreport*. 1994;5(18):2609–2612.
9. Fields RD. Nerve impulses regulate myelination through purinergic signalling. *Novartis Found Symp*. 2006;276:148–158.
10. Jeftinija S, Urban L. Repetitive stimulation induced potentiation of excitatory transmission in the rat dorsal horn: an in vitro study. *J Neurophysiol*. 1994;71(1):216–228.
11. Kadekaro M, Crane AM, Sokoloff L. Differential effects of electrical stimulation of sciatic nerve on metabolic activity in spinal cord and dorsal root ganglion in the rat. *Proc Natl Acad Sci U S A*. 1985;82(17):6010–6013.
12. Udina E, Furey M, Busch S, Silver J, Gordon T, Fouad K. Electrical stimulation of intact peripheral sensory axons in rats promotes outgrowth of their central projections. *Exp Neurol*. 2008;210(1):238–247.
13. Noonan L, Doiron B, Laing C, Longtin A, Turner RW. A dynamic dendritic refractory period regulates burst discharge in the electrosensory lobe of weakly electric fish. *J Neurosci*. 2003;23(4):1524–1534.
14. Berry MJ 2nd, Meister M. Refractoriness and neural precision. *J Neurosci*. 1998;18(6):2200–2211.
15. Chacron MJ, Longtin A, Maler L. Negative interspike interval correlations increase the neuronal capacity for encoding time-dependent stimuli. *J Neurosci*. 2001;21(14):5328–5343.
16. Luscher C, Streit J, Lipp P, Luscher HR. Action potential propagation through embryonic dorsal root ganglion cells in culture. II. Decrease of conduction reliability during repetitive stimulation. *J Neurophysiol*. 1994;72(2):634–643.
17. Momin A, McNaughton PA. Regulation of firing frequency in nociceptive neurons by pro-inflammatory mediators. *Exp Brain Res*. 2009;196(1):45–52.
18. Viana F, Bayliss DA, Berger AJ. Multiple potassium conductances and their role in action potential repolarization and repetitive firing behavior of neonatal rat hypoglossal motoneurons. *J Neurophysiol*. 1993;69(6):2150–2163.
19. Jung HY, Mickus T, Spruston N. Prolonged sodium channel inactivation contributes to dendritic action potential attenuation in hippocampal pyramidal neurons. *J Neurosci*. 1997;17(17):6639–6646.
20. Colbert CM, Magee JC, Hoffman DA, Johnston D. Slow recovery from inactivation of Na^+ channels underlies the activity-dependent attenuation of dendritic action potentials in hippocampal CA1 pyramidal neurons. *J Neurosci*. 1997;17(17):6512–6521.
21. Blair NT, Bean BP. Role of tetrodotoxin-resistant Na^+ current slow inactivation in adaptation of action potential firing in small-diameter dorsal root ganglion neurons. *J Neurosci*. 2003;23(32):10338–10350.
22. De Col R, Messlinger K, Carr RW. Conduction velocity is regulated by sodium channel inactivation in unmyelinated axons innervating the rat cranial meninges. *J Physiol*. 2008;586(4):1089–1103.
23. Vilin YY, Ruben PC. Slow inactivation in voltage-gated sodium channels: molecular substrates and contributions to channelopathies. *Cell Biochem Biophys*. 2001;35(2):171–190.
24. Wu Q, Henry JL. Delayed onset of changes in soma action potential genesis in nociceptive A-β DRG neurons in vivo in a rat model of osteoarthritis. *Mol Pain*. 2009;5:57.
25. Lawson SN, Crepps BA, Perl ER. Relationship of substance P to afferent characteristics of dorsal root ganglion neurones in guinea-pig. *J Physiol*. 1997;505(Pt 1):177–191.
26. Fang X, McMullan S, Lawson SN, Djouhri L. Electrophysiological differences between nociceptive and non-nociceptive dorsal root ganglion neurones in the rat in vivo. *J Physiol*. 2005;565(Pt 3):927–943.
27. Amir R, Devor M. Electrical excitability of the soma of sensory neurons is required for spike invasion of the soma, but not for through-conduction. *Biophys J*. 2003;84(4):2181–2191.
28. Ito M. An analysis of potentials recorded intracellularly from the spinal ganglion cell. *Jpn J Physiol*. 1959;9(1):20–32.
29. Djouhri L, Lawson SN. Aβ-fiber nociceptive primary afferent neurons: a review of incidence and properties in relation to other afferent A-fiber neurons in mammals. *Brain Res Brain Res Rev*. 2004;46(2):131–145.
30. Fukuoka T, Kobayashi K, Yamanaka H, Obata K, Dai Y, Noguchi K. Comparative study of the distribution of the α-subunits of voltage-gated sodium channels in normal and axotomized rat dorsal root ganglion neurons. *J Comp Neurol*. 2008;510(2):188–206.
31. Cummins TR, Aglieco F, Renganathan M, Herzog RI, Dib-Hajj SD, Waxman SG. $Na_v1.3$ sodium channels: rapid repriming and slow closed-state inactivation display quantitative differences after expression in a mammalian cell line and in spinal sensory neurons. *J Neurosci*. 2001;21(16):5952–5961.
32. Herzog RI, Cummins TR, Ghassemi F, Dib-Hajj SD, Waxman SG. Distinct repriming and closed-state inactivation kinetics of $Na_v1.6$ and $Na_v1.7$ sodium channels in mouse spinal sensory neurons. *J Physiol*. 2003;551(Pt 3):741–750.
33. Fleidervish IA, Friedman A, Gutnick MJ. Slow inactivation of Na^+ current and slow cumulative spike adaptation in mouse and guinea-pig neocortical neurones in slices. *J Physiol*. 1996;493(Pt 1):83–97.
34. Djouhri L, Dawbarn D, Robertson A, Newton R, Lawson SN. Time course and nerve growth factor dependence of inflammation-induced alterations in electrophysiological membrane properties in nociceptive primary afferent neurons. *J Neurosci*. 2001;21(22):8722–8733.
35. Fang X, Djouhri L, McMullan S, et al. Intense isolectin-B4 binding in rat dorsal root ganglion neurons distinguishes C-fiber nociceptors with broad action potentials and high $Na_v1.9$ expression. *J Neurosci*. 2006;26(27):7281–7292.
36. Ito M, Saiga M. The mode of impulse conduction through the spinal ganglion. *Jpn J Physiol*. 1959;9(1):33–42.
37. Lu GW, Miletic V. Responses of type A cat spinal ganglion neurons to repetitive stimulation of their central and peripheral processes. *Neuroscience*. 1990;39(1):259–270.
38. Luscher C, Streit J, Quadroni R, Luscher HR. Action potential propagation through embryonic dorsal root ganglion cells in culture. I. Influence of the cell morphology on propagation properties. *J Neurophysiol*. 1994;72(2):622–633.
39. Svaetichin G. Component analysis of action potentials from single neurons. *Exp Cell Res*. 1958;14(Suppl 5):234–261.
40. Creamer P, Lethbridge-Cejku M, Hochberg MC. Where does it hurt? Pain localization in osteoarthritis of the knee. *Osteoarthritis Cartilage*. 1998;6(5):318–323.
41. Appleton CT, McErlain DD, Henry JL, Holdsworth DW, Beier F. Molecular and histological analysis of a new rat model of experimental knee osteoarthritis. *Ann N Y Acad Sci*. 2007;1117:165–174.
42. McErlain DD, Appleton CT, Litchfield RB, et al. Study of subchondral bone adaptations in a rodent surgical model of OA using in vivo micro-computed tomography. *Osteoarthritis Cartilage*. 2008;16(4):458–469.
43. Appleton CT, McErlain DD, Pitelka V, et al. Forced mobilization accelerates pathogenesis: characterization of a preclinical surgical model of osteoarthritis. *Arthritis Res Ther*. 2007;9(1):R13.
44. Wu Q, Henry JL. Functional changes in muscle afferent neurones in an osteoarthritis model: implications for impaired proprioceptive performance. *PLoS One*. 2012;7(5):e36854.
45. Appleton CT, Pitelka V, Henry J, Beier F. Global analyses of gene expression in early experimental osteoarthritis. *Arthritis Rheum*. 2007;56(6):1854–1868.
46. Kean WF, Kean R, Buchanan WW. Osteoarthritis: symptoms, signs and source of pain. *Inflammopharmacology*. 2004;12(1):3–31.
47. Hawker GA, Stewart L, French MR, et al. Understanding the pain experience in hip and knee osteoarthritis – an OARSI/OMERACT initiative. *Osteoarthritis Cartilage*. 2008;16(4):415–422.

48. Nikolajsen L, Brandsborg B, Lucht U, Jensen TS, Kehlet H. Chronic pain following total hip arthroplasty: a nationwide questionnaire study. *Acta Anaesthesiol Scand*. 2006;50(4):495–500.
49. Caldwell JH, Schaller KL, Lasher RS, Peles E, Levinson SR. Sodium channel $Na_v1.6$ is localized at nodes of ranvier, dendrites, and synapses. *Proc Natl Acad Sci U S A*. 2000;97(10):5616–5620.
50. Hinson AW, Gu XQ, Dib-Hajj S, Black JA, Waxman SG. Schwann cells modulate sodium channel expression in spinal sensory neurons in vitro. *Glia*. 1997;21(4):339–349.
51. Waxman SG, Dib-Hajj S, Cummins TR, Black JA. Sodium channels and their genes: dynamic expression in the normal nervous system, dysregulation in disease states. *Brain Res*. 2000;886(1–2):5–14.
52. Wang LY, Gan L, Forsythe ID, Kaczmarek LK. Contribution of the $K_v3.1$ potassium channel to high-frequency firing in mouse auditory neurones. *J Physiol*. 1998;509(Pt 1):183–194.
53. Erisir A, Lau D, Rudy B, Leonard CS. Function of specific K^+ channels in sustained high-frequency firing of fast-spiking neocortical interneurons. *J Neurophysiol*. 1999;82(5):2476–2489.
54. Djouhri L, Newton R, Levinson SR, Berry CM, Carruthers B, Lawson SN. Sensory and electrophysiological properties of guinea-pig sensory neurones expressing $Na_v1.7$ (PN1) Na^+ channel α subunit protein. *J Physiol*. 2003;546(Pt 2):565–576.
55. Djouhri L, Fang X, Okuse K, Wood JN, Berry CM, Lawson SN. The TTX-resistant sodium channel $Na_v1.8$ (SNS/PN3): expression and correlation with membrane properties in rat nociceptive primary afferent neurons. *J Physiol*. 2003;550(Pt 3):739–752.
56. Fang X, Djouhri L, Black JA, Dib-Hajj SD, Waxman SG, Lawson SN. The presence and role of the tetrodotoxin-resistant sodium channel $Na_v1.9$ (NaN) in nociceptive primary afferent neurons. *J Neurosci*. 2002;22(17):7425–7433.
57. Rush AM, Brau ME, Elliott AA, Elliott JR. Electrophysiological properties of sodium current subtypes in small cells from adult rat dorsal root ganglia. *J Physiol*. 1998;511(Pt 3):771–789.
58. Black JA, Cummins TR, Plumpton C, et al. Upregulation of a silent sodium channel after peripheral, but not central, nerve injury in DRG neurons. *J Neurophysiol*. 1999;82(5):2776–2785.
59. Cummins TR, Waxman SG. Downregulation of tetrodotoxin-resistant sodium currents and upregulation of a rapidly repriming tetrodotoxin-sensitive sodium current in small spinal sensory neurons after nerve injury. *J Neurosci*. 1997;17(10):3503–3514.
60. Blair NT, Bean BP. Roles of tetrodotoxin (TTX)-sensitive Na^+ current, TTX-resistant Na^+ current, and Ca^{2+} current in the action potentials of nociceptive sensory neurons. *J Neurosci*. 2002;22(23):10277–10290.
61. Beyreuther BK, Freitag J, Heers C, Krebsfanger N, Scharfenecker U, Stohr T. Lacosamide: a review of preclinical properties. *CNS Drug Rev*. 2007;13(1):21–42.
62. Beyreuther BK, Geis C, Stohr T, Sommer C. Antihyperalgesic efficacy of lacosamide in a rat model for muscle pain induced by TNF. *Neuropharmacology*. 2007;52(5):1312–1317.